

Introduction

The emergence of coronavirus disease 2019 (COVID-19) as a pandemic in 2020 spurred many investigations on functional RNA structures in coronaviruses, particularly SARS coronavirus 2 (SARS-CoV-2) [1, 2, 3, 4, 5, 6, 7, 8, 9, 10]. Among the more unexpected findings was an RNA:RNA interaction between the frameshifting stimulation element (FSE) and another sequence up to 1,475 nt downstream, which the authors named the FSE-arch [3]. The FSE-arch was detected in infected cells using COMRADES [11] and proposed to comprise three nested long-range RNA:RNA interactions (Figure ??a): an outer 38 bp bulged stem spanning coordinates 13,370-14,842 (which encompasses the FSE); a middle 18 bp bulged stem spanning coordinates 13,533-14,673; and an inner 14 bp bulged stem spanning coordinates 13,580-14,552 [3]. We had discovered that the FSE folds into at least two alternative structures in infected cells, in roughly equal proportions, and that the predicted structure for one of them resembles the FSE-arch [10]. Because computational RNA structure prediction – even guided by chemical probing data – is unreliable for long RNA sequences especially [12], we sought stronger, hypothesis-driven evidence for the existence of the FSE-arch.

Chemical probing followed by mutational profiling is a common strategy for inferring secondary structures of RNA molecules [13, 14].

Here, we present a method to probe RNA–RNA interactions spanning hundreds to thousands of nucleotides, "Structure Ensemble Ablation by Reverse Complement Hybridization with Mutational Profiling" (SEARCH-MaP). To compute, compare, and deconvolute data from mutational profiling experiments (including SEARCH-MaP, DMS-MaPseq, and SHAPE-MaP), we introduce the software "Structure Ensemble Inference by Sequencing, Mutation Identification, and Clustering of RNA" (SEISMIC-RNA).

Results

Strategy of SEARCH-MaP and SEISMIC-RNA

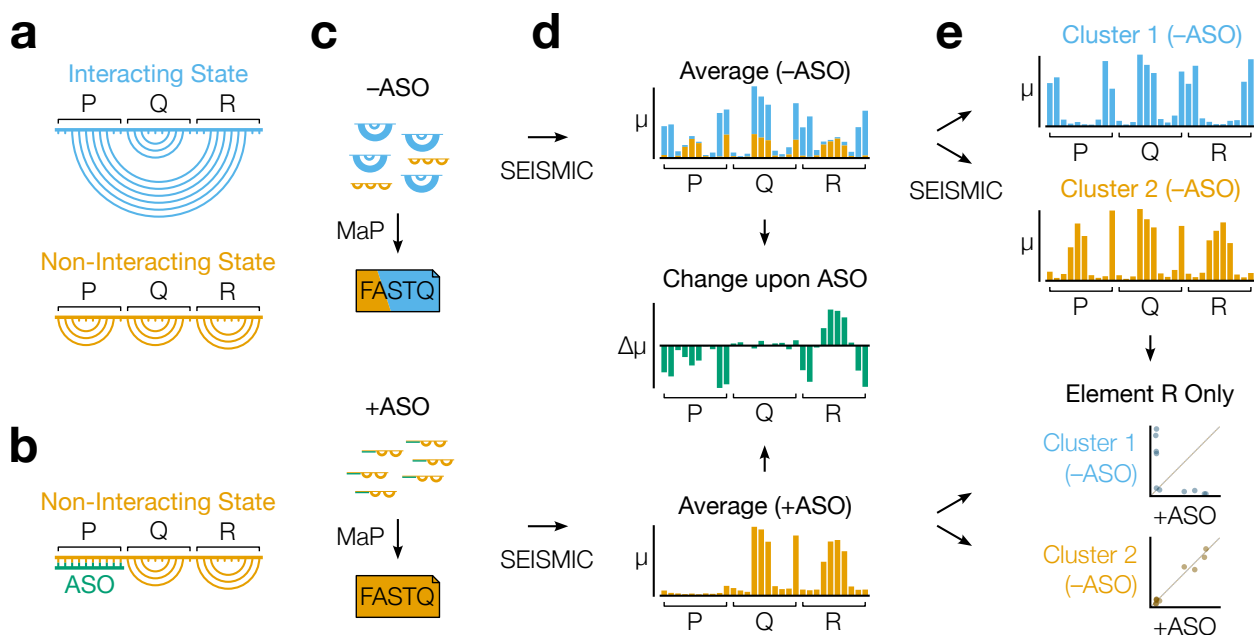


Figure 1: The strategy of SEARCH-MaP and SEISMIC-RNA. (a) This toy RNA is partitioned into three 10 nt elements (P, Q, and R) whose molecules exist in two structural states: one in which elements P and R interact (blue) and one in which they do not (orange). (b) Hybridizing an ASO (green) to element P blocks it from interacting with element R and forces all RNA molecules into the non-interacting state. (c) A SEARCH-MaP experiment entails separate chemical probing and mutational profiling (MaP) with (+ASO) and without (-ASO) the ASO, followed by sequencing to generate FASTQ files. The RNA molecules and FASTQ files use the same color scheme as in (a) and are illustrated/colored in proportion to their abundances in the ensemble. (d) Ensemble average mutational profiles with (+ASO) and without (-ASO) the ASO, computed with SEISMIC-RNA. The x-axis is the position in the RNA sequence; the y-axis is the fraction of mutations (μ) at the position. Each bar in the -ASO profile is drawn in two colors merely to illustrate how much each state contributes to each position; in a real experiment, states cannot be distinguished before clustering. The change upon ASO binding (green) indicates the difference in mutation fraction ($\Delta\mu$) between the +ASO and -ASO conditions. (e) Mutational profiles of two clusters (top) obtained by unmixing the -ASO ensemble in (d) using SEISMIC-RNA, and the scatter plot of the mutation rates in element R (bottom) between the +ASO ensemble average (x-axis) and each cluster (y-axis).

We illustrate SEARCH-MaP with an RNA comprising three elements (P, Q, and R) that folds into an ensemble of two structural states: one in which elements P and R interact, another in which they do not (Figure 1a). Searching for RNA–RNA interactions involving element P begins with hybridizing an antisense oligonucleotide (ASO) to element P, which blocks P–R base pairing and ablates the interacting state (Figure 1b). The perturbation is then detected by chemically probing with (+ASO) and without (–ASO) the ASO, followed by mutational profiling and sequencing, e.g. using DMS-MaPseq [13] (Figure 1c).

SEISMIC-RNA can detect RNA–RNA interactions by comparing the mutational profiles of +ASO and –ASO conditions. Theoretically, each structural state has its own mutational profile [15], but the mutational profile of a single state is not directly observable because all states are physically mixed during the experiment (Figure 1c, top). Instead, the directly observable mutational profile is the "ensemble average" – the average of the states' (unobserved) mutational profiles, weighted by the states' (unobserved) proportions (Figure 1d, top). Because the structures – and therefore mutational profiles – of element R differ between the interacting and non-interacting states, the ensemble averages over element R also differ between the +ASO and –ASO conditions (Figure 1d, middle). However, this is not the case for element Q, which has the same secondary structure in both states (Figure 1d, middle). Therefore, one can deduce that P interacts with R – but not with Q – because hybridizing an ASO to P alters the mutational profile of R but not of Q.

After identifying RNA–RNA interactions, SEISMIC-RNA can also determine the mutational profiles of the interacting and non-interacting states – even if their secondary structures are unknown. Inferring mutational profiles for the interacting and non-interacting states requires unmixing the –ASO ensemble into two clusters of RNA molecules (Figure 1e, top). Each cluster has its own mutational profile and corresponds to one structural state, but which cluster corresponds to the interacting (or non-interacting) state is not yet known. The non-interacting state has a mutational profile similar to that of the +ASO ensemble average, since the ASO forces the RNA into the non-interacting state. Therefore,

over the element (in this case, R) that interacts with the ASO-bound element, the cluster that correlates better with the +ASO ensemble average is the non-interacting state (Figure 1e, bottom). Using this technique, one can deduce that Cluster 2 corresponds to the non-interacting state, and Cluster 1 to the interacting state.

Frameshift stimulating elements of multiple coronaviruses form long-range RNA–RNA interactions

Within the genomes of many RNA viruses, long-range RNA–RNA interactions regulate core processes such as viral protein synthesis [16]. In SARS coronavirus 2 (SARS-CoV-2), the frameshift stimulating element (FSE) base pairs with another genomic element over 1,000 nt downstream [3]. For its length, this RNA–RNA interaction appears surprisingly favorable, forming in approximately half of the genomic RNA molecules within infected cells [10]. Although the FSE is essential for synthesizing five viral proteins including the RNA polymerase, the function (if any) of the long-range interaction it forms remains unknown [17].

We hypothesized that if the long-range interaction is functional, then other SARS-related viruses – and potentially more distantly related coronaviruses – would feature similar long-range interactions involving their FSEs. To test this hypothesis, we performed SEARCH-MaP with FSE-targeted ASOs on 1,799 nt segments from eight selected coronaviruses.

Computational and experimental screening identifies eight coronaviruses with potential long-range interactions

As of December 2021, the NCBI Reference Sequence Database [18] contained sixty-two complete genomes of coronaviruses. To focus on those likely to have long-range interactions involving the FSE, we predicted the likelihood that each base in a 2,000 nt section surrounding the FSE would pair with a base in the FSE. Based on these predicted inter-

actions (SFIG), we selected ten coronaviruses (including SARS-CoV-2) for further study – at least one from each genus. Within the genus *Betacoronavirus*, we included all three of the SARS-related viruses – SARS coronaviruses 1 (NC_004718.3) and 2 (NC_045512.2) and bat coronavirus BM48-31 (NC_014470.1) – because they clustered into their own structural outgroup, distinct from all other coronaviruses. The other three strains of *Betacoronavirus* that we selected were MERS coronavirus (NC_019843.3) with a predicted interaction at positions 510-530; and human coronavirus OC43 (NC_006213.1) and murine hepatitis virus strain A59 (NC_048217.1), both with a predicted upstream interaction at positions 10-20. We selected two strains of *Alphacoronavirus*: transmissible gastroenteritis virus (NC_038861.1) and bat coronavirus 1A (NC_010437.1), predicted to have interactions at positions 440-460 and 350-360, respectively. Avian infectious bronchitis virus strain Beaudette (NC_001451.1) – a strain of *Gammacoronavirus* – was predicted to have a strong interaction at positions 330-350, while common moorhen coronavirus HKU21 (NC_016996.1) was the species of *Deltacoronavirus* with the most promising FSE interactions.

We reasoned that if an FSE does interact with a distant RNA element, then removing that element by truncating the RNA would break the interaction, causing a structural change in the FSE that could be detected through chemical probing. For each of the ten coronaviruses that passed the computational screen, we *in vitro* transcribed and performed DMS-MaPseq [13] on both a 239 nt ("short") segment comprising the FSE and minimal flanking sequences and a 1,799 nt ("long") segment encompassing the FSE and all sites with which it was predicted to interact. All coronaviruses except for human coronavirus OC43 and MERS coronavirus showed differences in their DMS reactivity profiles between the short and long segments (SFIG), suggesting long-range interactions between the FSE and another element within the long segment.

SEARCH-MaP reveals long-range interactions involving the FSE in four coronaviruses

To determine whether the FSE forms a long-range interaction with another RNA element – and if so, which element – in each coronavirus, we performed SEARCH-MaP on the 1,799 nt RNA segment using FSE-targeted ASOs. We computed the Spearman correlation using a sliding window between the DMS reactivities with and without ASOs (Figure 2). [HOW MANY] coronaviruses

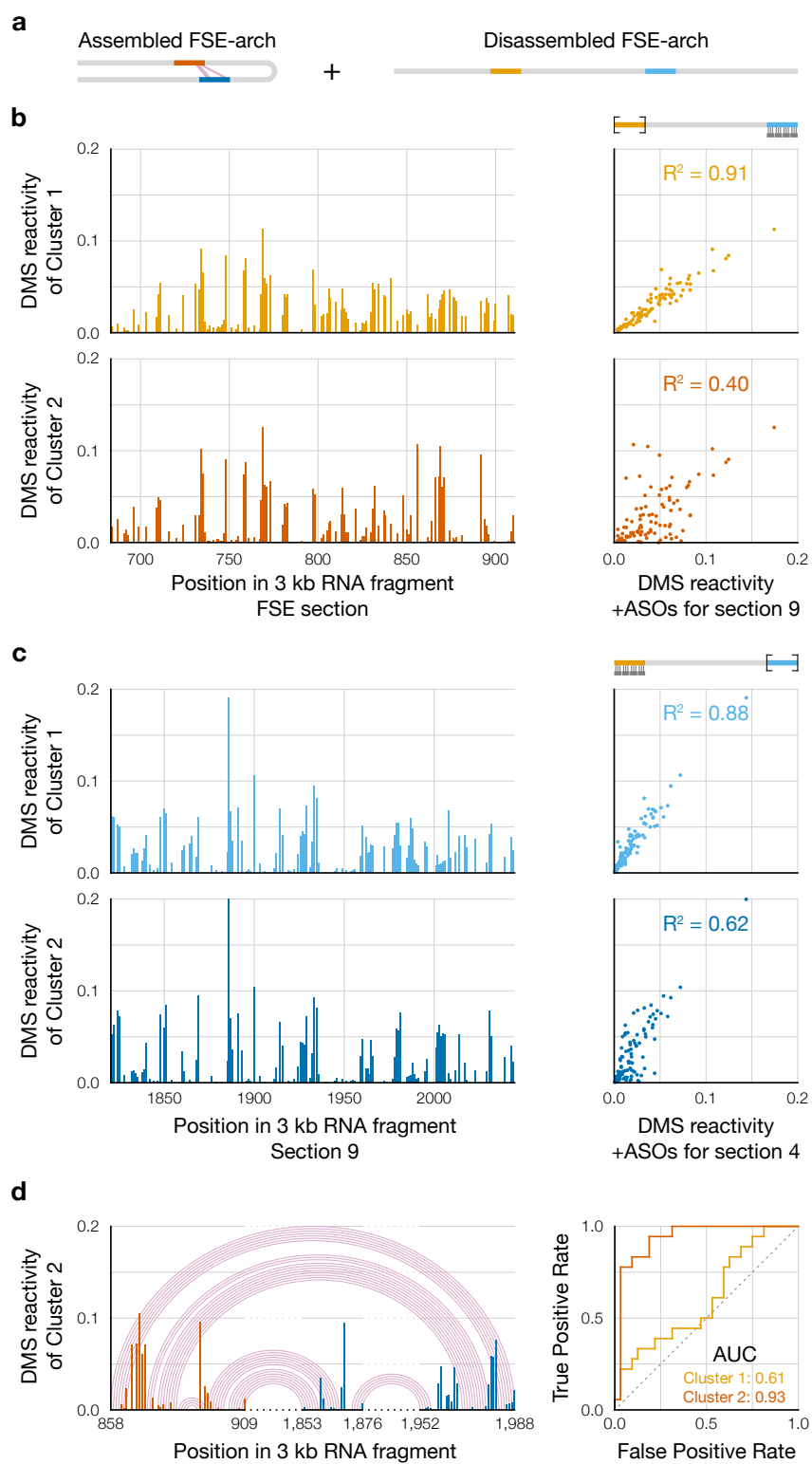


Figure 2:

Discussion

In this work, we developed SEARCH-MaP and SEISMIC and applied them jointly to detect structural ensembles involving long-range RNA:RNA interactions in SARS-CoV-2 and other coronaviruses. This study is certainly not the first to perturb RNA structure with ASOs, nor even the first to use DMS-MaPseq to quantify the structural changes upon binding ASOs to SARS-CoV-2 RNA [19]. But while this previous study examined local structural perturbations caused by binding an ASO, we show that we can detect changes in the structure at more distant locations in an RNA molecule that interact with the nucleotides bound by an ASO.

SEARCH-MaP bears conceptual similarity to another method, mutate-and-map read out through next-generation sequencing (M2-seq) [20]. Both involve perturbing one region of an RNA molecule (in the case of M2-seq, by pre-installing mutations through error-prone PCR) and measuring the effects on other bases in the RNA using chemical probing. The major differences are the precision and scale of the interactions identified, as well as the throughput. M2-seq can pinpoint interactions down to the resolution of a single base pair, and is thus more precise than SEARCH-MaP. However, SEARCH-MaP is capable of finding interactions over a much longer range because M2-seq requires the interacting bases to be in the same Illumina sequencing read. Within this length limit, one M2-seq experiment can theoretically find all pairwise interactions between bases, while one SEARCH-MaP experiment can find only interactions that involve the region to which the ASOs were hybridized.

Another limitation of SEARCH-MaP as presented here is that it cannot distinguish between direct and indirect interactions. If RNA segment A interacts with segment B, while B interacts with both segment A and C, then hybridizing an ASO to segment A would perturb the structure of B, which could consequentially perturb the structure of C. Hence, C would appear to interact with A, even though this interaction is indirect, through B. One possible workaround (not shown in this study) would be to mutate or hybridize an ASO to

segment B, and then repeat the experiment with hybridizing an ASO to segment A. If the interaction between A and C is direct, then C should still be perturbed even when segment B is incapable of interacting with A or C. But if B mediates an indirect interaction between A and C, then disrupting B should eliminate the apparent interaction between A and C.

Functional long-range interactions up to four kilobases involving an FSE have been found previously in two plant viruses [21, 22]. In both cases, frameshifting required the long-range interaction, suggesting that this interaction enables negative feedback on synthesis of viral RNA polymerase [21]. When polymerase levels are low, the interaction would form and stimulate frameshifting, which is needed to synthesize RNA polymerase. Once the polymerase had accumulated, it would begin to replicate the genomic RNA; in its passage from the genomic 3' end to the 5' end, it would disrupt the 3' side of the long-range interaction, attenuating frameshifting and reducing synthesis of more polymerase.

However, this strategy cannot be the role, if any, of the long-range interactions in coronaviruses. Unlike in the two plant viruses, a long-range interaction is not required to stimulate frameshifting in coronaviruses: numerous studies have shown that even the isolated FSE can cause 15 - 40% of ribosomes to frameshift [23, 24, 25, 10, 26, 27, 28]. In coronaviruses, the long-range interaction is not only unnecessary for frameshifting but also may even attenuate it, given that in SARS-CoV-2, the FSE-arch and the frameshift-stimulating pseudoknot seem to be mutually exclusive. Moreover, coronaviruses partition translation and RNA synthesis into two different cellular compartments (the cytosol and the double-membrane vesicles, respectively) [29], so structural changes induced by RNA polymerases would not be seen by ribosomes.

The functions of these long-range interactions involving the FSE in coronaviruses remain mysterious. However, given that they occur in multiple coronaviruses across at least two genera, it seems reasonable that they could play a role in the viral life cycle, possibly by affecting the rate of frameshifting. Further research may reveal new mechanisms of translational regulation in coronaviruses via long-range RNA:RNA interactions.

Methods

Screening coronavirus long-range interactions computationally

All coronaviruses with reference genomes in the NCBI Reference Sequence Database [18] were searched for using the following query:

```
refseq[filter] AND ("Alphacoronavirus"[Organism] OR  
                    "Betacoronavirus"[Organism] OR  
                    "Gammacoronavirus"[Organism] OR  
                    "Deltacoronavirus"[Organism])
```

The complete record of every reference genome was downloaded both in FASTA format (for the reference sequence) and in Feature Table format (for feature locations). The location of the frameshift stimulating element (FSE) in each genome was estimated from the feature table, and the nearest instance of TTAAAC was used as the slippery site, using a custom Python script. The 2,000 nt segment beginning 100 nt upstream of and ending 1,893 nt downstream of the slippery site was used for predicting long-range interactions involving the FSE. Genomes with ambiguous nucleotides (e.g. N) in this segment were discarded. For each coronavirus genome, up to 100 secondary structure models of the 2,000 nt segment were generated using Fold version 6.3 from RNAstructure [30] with $-M$ 100 and otherwise default parameters. Then, for each position, the fraction of models for the coronavirus in which the base at the position paired with any other base between positions 101 (the first base of the slippery sequence) and 250 was calculated using a custom Python script. The coronaviruses were clustered by their fraction vectors using the unweighted pair group method with arithmetic mean (UPGMA) and a euclidean distance metric, implemented in Seaborn version 0.11 [31] and SciPy version 1.7 [32]. The resulting hierarchically-clustered

heatmap was examined manually to select coronaviruses based on the prominence of potential long-range interactions with the FSE (relatively large fractions far from positions 101-250).

References

- [1] Ramya Rangan, Ivan N. Zheludev, Rachel J. Hagey, Edward A. Pham, Hannah K. Wayment-Steele, Jeffrey S. Glenn, and Rhiju Das. Rna genome conservation and secondary structure in sars-cov-2 and sars-related viruses: a first look. *RNA*, 26(8):937–959, 2020.
- [2] Ilaria Manfredonia, Chandran Nithin, Almudena Ponce-Salvatierra, Pritha Ghosh, Tomasz K. Wirecki, Tycho Marinus, Natacha S. Ogando, Eric J. Snijder, Martijn J. van Hemert, Janusz M. Bujnicki, and Danny Incarnato. Genome-wide mapping of sars-cov-2 rna structures identifies therapeutically-relevant elements. *Nucleic Acids Research*, 48:12436–12452, 2020.
- [3] Omer Ziv, Jonathan Price, Lyudmila Shalamova, Tsveta Kamenova, Ian Goodfellow, Friedemann Weber, and Eric A. Miska. The short- and long-range rna-rna interactome of sars-cov-2. *Molecular Cell*, 80:1067–1077.e5, 12 2020.
- [4] Lei Sun, Pan Li, Xiaohui Ju, Jian Rao, Wenze Huang, Lili Ren, Shaojun Zhang, Tuanlin Xiong, Kui Xu, Xiaolin Zhou, Mingli Gong, Eric Miska, Qiang Ding, Jianwei Wang, and Qiangfeng Cliff Zhang. In vivo structural characterization of the sars-cov-2 rna genome identifies host proteins vulnerable to repurposed drugs. *Cell*, 184:1865–1883.e20, 2021.
- [5] Yan Zhang, Kun Huang, Dejian Xie, Jian You Lau, Wenlong Shen, Ping Li, Dong Wang, Zhong Zou, Shu Shi, Hongguang Ren, Youliang Wang, Youzhi Mao, Meilin Jin, Grzegorz Kudla, and Zhihu Zhao. In vivo structure and dynamics of the sars-cov-2 rna genome. *Nature Communications*, 12:5695, 9 2021.
- [6] Nicholas C. Huston, Han Wan, Madison S. Strine, Rafael de Cesaris Araujo Tavares, Craig B. Wilen, and Anna Marie Pyle. Comprehensive in vivo secondary structure of the sars-cov-2 genome reveals novel regulatory motifs and mechanisms. *Molecular Cell*, 81, 2021.
- [7] Ramya Rangan, Andrew M. Watkins, Jose Chacon, Rachael Kretsch, Wipapat Kladwang, Ivan N. Zheludev, Jill Townley, Mats Rynge, Gregory Thain, and Rhiju Das. De novo 3d models of sars-cov-2 rna elements from consensus experimental secondary structures. *Nucleic Acids Research*, 49:3092–3108, 4 2021.

- [8] Edoardo Morandi, Ilaria Manfredonia, Lisa M. Simon, Francesca Anselmi, Martijn J. van Hemert, Salvatore Oliviero, and Danny Incarnato. Genome-scale deconvolution of rna structure ensembles. *Nature Methods*, 18:249–252, 2 2021.
- [9] Siwy Ling Yang, Louis DeFalco, Danielle E. Anderson, Yu Zhang, Jong Ghut Ashley Aw, Su Ying Lim, Xin Ni Lim, Kiat Yee Tan, Tong Zhang, Tanu Chawla, Yan Su, Alexander Lezhava, Andres Merits, Lin Fa Wang, Roland G. Huber, and Yue Wan. Comprehensive mapping of sars-cov-2 interactions in vivo reveals functional virus-host interactions. *Nature Communications*, 12, 2021.
- [10] Tammy C.T. Lan, Matty F. Allan, Lauren E. Malsick, Jia Z. Woo, Chi Zhu, Fengrui Zhang, Stuti Khandwala, Sherry S.Y. Nyeo, Yu Sun, Junjie U. Guo, Mark Bathe, Anders Nää, Anthony Griffiths, and Silvi Rouskin. Secondary structural ensembles of the sars-cov-2 rna genome in infected cells. *Nature Communications*, 13:1128, 3 2022.
- [11] Omer Ziv, Marta M. Gabryelska, Aaron T.L. Lun, Luca F.R. Gebert, Jessica Sheu-Gruttadauria, Luke W. Meredith, Zhong Yu Liu, Chun Kit Kwok, Cheng Feng Qin, Ian J. MacRae, Ian Goodfellow, John C. Marioni, Grzegorz Kudla, and Eric A. Miska. Comrades determines in vivo rna structures and interactions. *Nature Methods*, 15:785–788, 9 2018.
- [12] Sharon Aviran and Danny Incarnato. Computational approaches for rna structure ensemble deconvolution from structure probing data. *Journal of Molecular Biology*, 434:167635, 9 2022.
- [13] Meghan Zubradt, Paromita Gupta, Sitara Persad, Alan M. Lambowitz, Jonathan S. Weissman, and Silvi Rouskin. Dms-mapseq for genome-wide or targeted rna structure probing in vivo. *Nature Methods*, 2254:219–238, 2016.
- [14] Nathan A. Siegfried, Steven Busan, Gregory M. Rice, Julie A.E. Nelson, and Kevin M. Weeks. Rna motif discovery by shape and mutational profiling (shape-map). *Nature methods*, 2014.
- [15] Chringma Sherpa, Jason W. Rausch, Stuart F.J. Le Grice, Marie Louise Hammarskjold, and David Rekosh. The hiv-1 rev response element (rre) adopts alternative conformations that promote different rates of virus replication. *Nucleic Acids Research*, 43:4676–4686, 3 2015.
- [16] Beth L. Nicholson and K. Andrew White. Functional long-range rna–rna interactions in positive-strand rna viruses. *Nature Reviews Microbiology*, 12:493–504, 6 2014.
- [17] Matthew F. Allan, Amir Brivanlou, and Silvi Rouskin. Rna levers and switches controlling viral gene expression. *Trends in Biochemical Sciences*, 48, 2023.
- [18] Nuala A. O’Leary, Mathew W. Wright, J. Rodney Brister, Stacy Ciufu, Diana Haddad, Rich McVeigh, Bhanu Rajput, Barbara Robbertse, Brian Smith-White, Danso Ako-Adjei, Alexander Astashyn, Azat Badretdin, Yiming Bao, Olga Blinkova, Vyacheslav Brover, Vyacheslav Chetvernin, Jinna Choi, Eric Cox, Olga Ermolaeva, Catherine M.

Farrell, Tamara Goldfarb, Tripti Gupta, Daniel Haft, Eneida Hatcher, Wratkan Hlavina, Vinita S. Joardar, Vamsi K. Kodali, Wenjun Li, Donna Maglott, Patrick Master-son, Kelly M. McGarvey, Michael R. Murphy, Kathleen O'Neill, Shashikant Pujar, Sanjida H. Rangwala, Daniel Rausch, Lillian D. Riddick, Conrad Schoch, Andrei Shkeda, Susan S. Storz, Hanzhen Sun, Francoise Thibaud-Nissen, Igor Tolstoy, Raymond E. Tully, Anjana R. Vatsan, Craig Wallin, David Webb, Wendy Wu, Melissa J. Landrum, Avi Kimchi, Tatiana Tatusova, Michael DiCuccio, Paul Kitts, Terence D. Murphy, Kim D. Pruitt, O'Leary NA, Wright MW, Brister JR, Ciufo S, Haddad Haft D, McVeigh R, Robertse Rajput B, Robertse Rajput B, Smith-White B, Ako-Adjei D, Astashyn A, Badret-din A, Bao Y, Blinkova O, Brover V, Chetvernin V, Choi J, Cox E, Ermolaeva O, Farrell CM, Goldfarb Gupta T, Goldfarb Gupta T, Haddad Haft D, Hatcher E, Hlavina W, Joardar VS, Kodali VK, Li W, Maglott D, Masterson P, McGarvey KM, Murphy MR, O'Neill K, Pujar S, Rangwala SH, Rausch D, Riddick LD, Schoch C, Shkeda A, Storz SS, Sun H, Thibaud-Nissen F, Tolstoy I, Tully RE, Vatsan AR, Wallin C, Webb D, Wu W, Landrum MJ, Kimchi A, Tatusova T, DiCuccio M, Kitts P, Murphy TD, and Pruitt KD. Reference sequence (refseq) database at ncbi: current status, taxonomic expansion, and functional annotation. *Nucleic Acids Research*, 44:D733–D745, 2016.

- [19] Chi Zhu, Justin Y. Lee, Jia Z. Woo, Lei Xu, Xammy Nguyenla, Livia H. Yamashiro, Fei Ji, Scott B. Biering, Erik Van Dis, Federico Gonzalez, Douglas Fox, Eddie Wehri, Arjun Rustagi, Benjamin A. Pinsky, Julia Schaletzky, Catherine A. Blish, Charles Chiu, Eva Harris, Ruslan I. Sadreyev, Sarah Stanley, Sakari Kauppinen, Silvi Rouskin, and Anders M. Näär. An intranasal aso therapeutic targeting sars-cov-2. *Nature Communications*, 13:4503, 12 2022.
- [20] Clarence Y. Cheng, Wipapat Kladwang, Joseph D. Yesselman, and Rhiju Das. Rna structure inference through chemical mapping after accidental or intentional mutations. *Proceedings of the National Academy of Sciences of the United States of America*, 114:9876–9881, 9 2017.
- [21] Jennifer K. Barry and W. Allen Miller. A -1 ribosomal frameshift element that requires base pairing across four kilobases suggests a mechanism of regulating ribosome and replicase traffic on a viral rna. *Proceedings of the National Academy of Sciences of the United States of America*, 99:11133–11138, 8 2002.
- [22] Yuri Tajima, Hiro oki Iwakawa, Masanori Kaido, Kazuyuki Mise, and Tetsuro Okuno. A long-distance rna–rna interaction plays an important role in programmed - 1 ribosomal frameshifting in the translation of p88 replicase protein of red clover necrotic mosaic virus. *Virology*, 417:169–178, 8 2011.
- [23] Pramod R. Bhatt, Alain Scaiola, Gary Loughran, Marc Leibundgut, Annika Kratzel, Romane Meurs, René Dreos, Kate M. O'Connor, Angus McMillan, Jeffrey W. Bode, Volker Thiel, David Gatfield, John F. Atkins, and Nenad Ban. Structural basis of ribosomal frameshifting during translation of the sars-cov-2 rna genome. *Science*, 372:1306–1313, 5 2021.

- [24] Hafeez S. Haniff, Yuquan Tong, Xiaohui Liu, Jonathan L. Chen, Blessy M. Suresh, Ryan J. Andrews, Jake M. Peterson, Collin A. O’Leary, Raphael I. Benhamou, Walter N. Moss, and Matthew D. Disney. Targeting the sars-cov-2 rna genome with small molecule binders and ribonuclease targeting chimera (ribotac) degraders. *ACS Central Science*, 6:1713–1721, 2020.
- [25] Jamie A. Kelly, Alexandra N. Olson, Krishna Neupane, Sneha Munshi, Josue San Eme-terio, Lois Pollack, Michael T. Woodside, and Jonathan D. Dinman. Structural and func-tional conservation of the programmed -1 ribosomal frameshift signal of sars coron-avirus 2 (sars-cov-2). *Journal of Biological Chemistry*, 295:10741–10748, 7 2020.
- [26] Ewan P. Plant, Rasa Rakauskaitė, Deborah R. Taylor, and Jonathan D. Dinman. Achiev-ing a golden mean: Mechanisms by which coronaviruses ensure synthesis of the cor-rect stoichiometric ratios of viral proteins. *Journal of Virology*, 84:4330–4340, 2010.
- [27] Yu Sun, Laura Abriola, Rachel O. Niederer, Savannah F. Pedersen, Mia M. Alfajaro, Val-ter Silva Monteiro, Craig B. Wilen, Ya-Chi Ho, Wendy V. Gilbert, Yulia V. Surovtseva, Brett D. Lindenbach, and Junjie U. Guo. Restriction of sars-cov-2 replication by tar-geting programmed -1 ribosomal frameshifting. *Proceedings of the National Academy of Sciences of the United States of America*, 118:e2023051118, 6 2021.
- [28] Kaiming Zhang, Ivan N. Zheludev, Rachel J. Hagey, Raphael Haslecker, Yixuan J. Hou, Rachael Kretsch, Grigore D. Pintilie, Ramya Rangan, Wipapat Kladwang, Shanshan Li, Marie Teng Pei Wu, Edward A. Pham, Claire Bernardin-Souibgui, Ralph S. Baric, Timo-thy P. Sheahan, Victoria D’Souza, Jeffrey S. Glenn, Wah Chiu, and Rhiju Das. Cryo-em and antisense targeting of the 28-kda frameshift stimulation element from the sars-cov-2 rna genome. *Nature Structural & Molecular Biology*, 28:747–754, 8 2021.
- [29] Georg Wolff, Charlotte E. Melia, Eric J. Snijder, and Montserrat Bárcena. Double-membrane vesicles as platforms for viral replication. *Trends in Microbiology*, 28:1022–1033, 12 2020.
- [30] David H. Mathews, Matthew D. Disney, Jessica L. Childs, Susan J. Schroeder, Michael Zuker, and Douglas H. Turner. Incorporating chemical modification constraints into a dynamic programming algorithm for prediction of rna secondary structure. *Proceed-ings of the National Academy of Sciences*, 101:7287–7292, 5 2004.
- [31] Michael Waskom. seaborn: statistical data visualization. *Journal of Open Source Soft-ware*, 6, 2021.
- [32] Pauli Virtanen, Ralf Gommers, Travis E. Oliphant, Matt Haberland, Tyler Reddy, David Cournapeau, Evgeni Burovski, Pearu Peterson, Warren Weckesser, Jonathan Bright, Stéfan J. van der Walt, Matthew Brett, Joshua Wilson, K. Jarrod Millman, Nikolay May-orov, Andrew R. J. Nelson, Eric Jones, Robert Kern, Eric Larson, C J Carey, İlhan Polat, Yu Feng, Eric W. Moore, Jake VanderPlas, Denis Laxalde, Josef Perktold, Robert Cim-rman, Ian Henriksen, E. A. Quintero, Charles R. Harris, Anne M. Archibald, Antônio H. Ribeiro, Fabian Pedregosa, Paul van Mulbregt, and SciPy 1.0 Contributors. SciPy 1.0:

Fundamental Algorithms for Scientific Computing in Python. *Nature Methods*, 17:261–272, 2020.